

Designing Limited-EIRP, Long-distance Links for Water Management Networks Using Polarization Diversity and Redundant Routing Paths

Antonios G. Dimitriou
School of ECE,
Aristotle Univ. of Thessaloniki
Thessaloniki, Greece 54124
antodimi@auth.gr

Dimitris Ntilis
School of ECE,
Technical Univ. of Crete
Kounoupidiana Campus
Chania, Greece 73100
dntilis@hotmail.com

Panagiotis Oikonomakos
School of ECE,
Technical Univ. of Crete
Kounoupidiana Campus
Chania, Greece 73100
panos.oikonomakos@gmail.com

Antonios Inglezakis
School of ECE,
Technical Univ. of Crete
Kounoupidiana Campus
Chania, Greece 73100
aigglezakis@softnet.tuc.gr

Vasileios Papadakis
Network Operation Center,
Technical Univ. of Crete
Kounoupidiana Campus
Chania, Greece 73100
ikaros.05@ict.tuc.gr

Aggelos Bletsas
School of ECE,
Technical Univ. of Crete
Kounoupidiana Campus
Chania, Greece 73100
aggelos@telecom.tuc.gr

ABSTRACT

This work presents the design of a long-distance wireless sensor network (WSN) for city-wide water management. The network consists of several nodes, located at specific points of interest, with intermediate distances that could exceed 4.5 kilometers. The maximum equivalent isotropic radiated power (EIRP) constraints at the utilized frequency of 2.4GHz require non-trivial antenna and network design. It is found that orthogonal polarization in a 2×2 multi-input multi-output (MIMO) system can improve long-distance links against fading. Furthermore, ensuring point-to-multipoint visibility among the nodes greatly reduces outage probability for each long-distance link.

Keywords

MIMO, propagation, orthogonal polarization, Rician fading

1. INTRODUCTION

We have developed a low-cost and large-scale pilot wireless sensor network (WSN) for city-wide water management that augments the existing monitoring and management functionality of the municipal enterprise of Chania, Crete, Greece. Water-level measurement is conducted by a prototype low-cost capacitive sensor. IEEE 802.11b/g cards are installed for wireless data transmission. Water-tanks are mainly located around the city and at large distances from each other (in the order of 1.5km-5km), as shown in Figure 1. Max-

imum EIRP is 20dBm, while 802.11 radio receiver's sensitivity for the smallest supported rate is in the order of -90dBm. These constraints require the implementation of sophisticated techniques to minimize the outage probability at any receiving node of the network.

All water tanks are located around the city in a rural environment, characterized by dense foliage; mainly olive-trees (see the photo of Figure 2). The locations of the nodes of the network are fixed and coincide with the locations of the tanks. Due to the power constraints of the problem (maximum EIRP vs receiver's sensitivity) and the large distances among tanks, only nodes that satisfy line-of-sight (LOS) conditions can communicate. We exploit two properties, in order to shield our network against destructive fading: *i*) the field that impinges on foliage is depolarized [1]-[5], *ii*) the

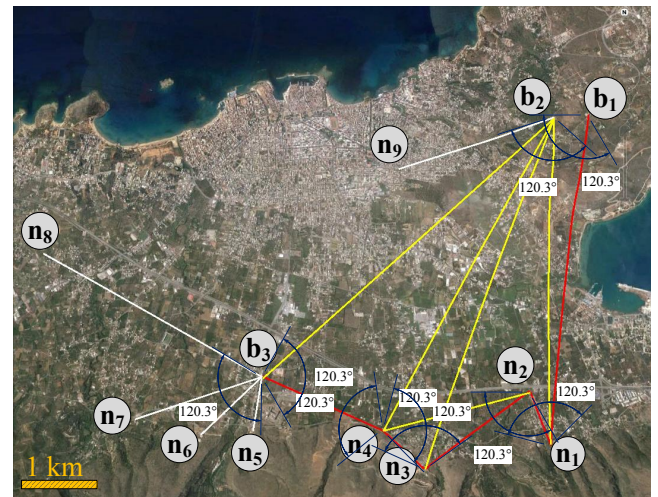


Figure 1: Topology of the wireless sensor network of water-tanks.

imum EIRP is 20dBm, while 802.11 radio receiver's sensitivity for the smallest supported rate is in the order of -90dBm. These constraints require the implementation of sophisticated techniques to minimize the outage probability at any receiving node of the network.

All water tanks are located around the city in a rural environment, characterized by dense foliage; mainly olive-trees (see the photo of Figure 2). The locations of the nodes of the network are fixed and coincide with the locations of the tanks. Due to the power constraints of the problem (maximum EIRP vs receiver's sensitivity) and the large distances among tanks, only nodes that satisfy line-of-sight (LOS) conditions can communicate. We exploit two properties, in order to shield our network against destructive fading: *i*) the field that impinges on foliage is depolarized [1]-[5], *ii*) the

Permission to make digital or hard copies of all or part of this work for personal or classroom use is granted without fee provided that copies are not made or distributed for profit or commercial advantage and that copies bear this notice and the full citation on the first page. To copy otherwise, to republish, to post on servers or to redistribute to lists, requires prior specific permission and/or a fee.

CySWater'15 April 13-16, 2015, Seattle, WA, USA
Copyright 2015 ACM 978-1-4503-3485-3/15/04 ...\$15.00.
<http://dx.doi.org/10.1145/2738935.2738944>.



Figure 2: Photo of the area of the network.

outage probability of a given node is reduced by increasing the possible paths of information-flow.

The 1st property is exploited by implementing polarization diversity at each node, as shown in Figures 3, 5. We transmit the same information (the measured water-tank level) from two orthogonally polarized antennas. The field at the receiving antenna for each polarization is given as the phase sum of a strong LOS component and several randomly polarized contributions of smaller magnitude coming from foliage. Therefore, the field for each polarization can be stochastically quantified by an appropriate Rician probability density function. Furthermore, due to the de-polarization effects of foliage, the two distributions (for the two polarizations) can be considered independent, thus greatly reducing the probability that both links suffer from destructive fading as will be demonstrated.

We take advantage of the 2nd property by using 120° sector antennas at the nodes. This ensures redundant paths for the information to flow around the network. Therefore, even if both orthogonal links of a point-to-point (P2P) connection are temporarily below the desired threshold, information may still be directed towards the backbone network from alternative paths.

A block diagram representing the functionality of each node is given in Figure 3.

2. ORTHOGONAL POLARIZATION ABOVE TREES

Part of the propagation area is illustrated in Figure 2. The paths that are expected to link the transmitter and the receiver are shown in Figure 4. At the receiver, there is a strong LOS field and several weaker contributions arriving from trees, located in the area between the transmitter and the receiver. The existence of the trees is of great importance for the success of the proposed diversity-polarization technique. The electromagnetic field induces currents in the foliage which are randomly oriented. As a consequence, the resultant scattered field is randomly polarized with respect to the incident field [1]-[5]. As this process takes place for both polarizations of the transmitted field and each polarization interacts differently with the branches and leaves, the scattered rays from foliage for the two polarizations are uncorrelated. Notice that this is not the case for the two-ray model [6] (an infinite plane is assumed between the two an-

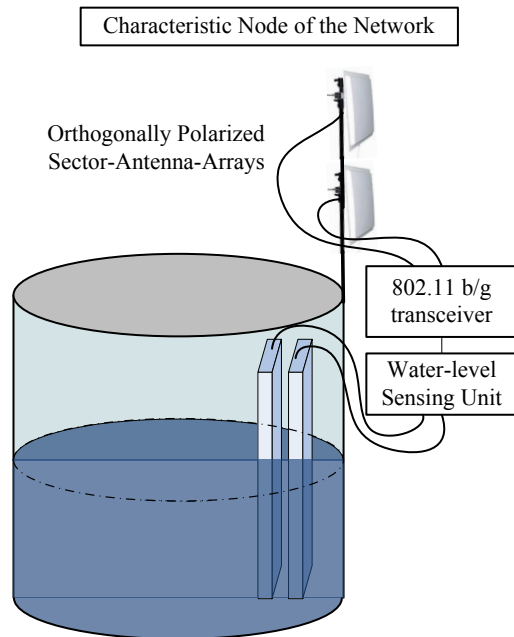


Figure 3: Block diagram representing the functionality of any sensor node of the network.

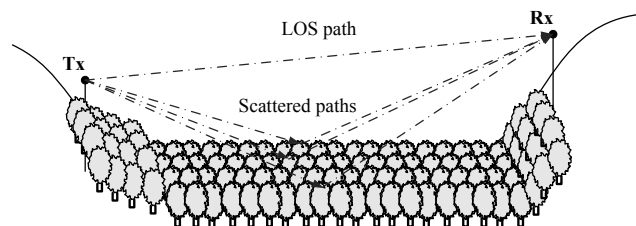


Figure 4: Representation of the propagation paths between the transmitter and the receiver.

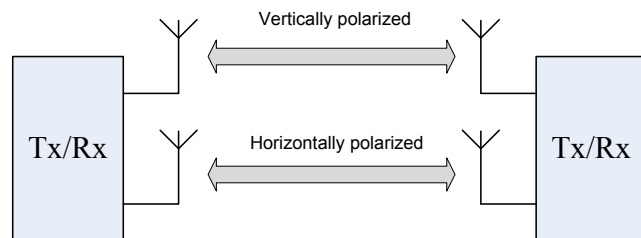


Figure 5: A pair of orthogonally polarized antenna-arrays is considered at each transceiver.

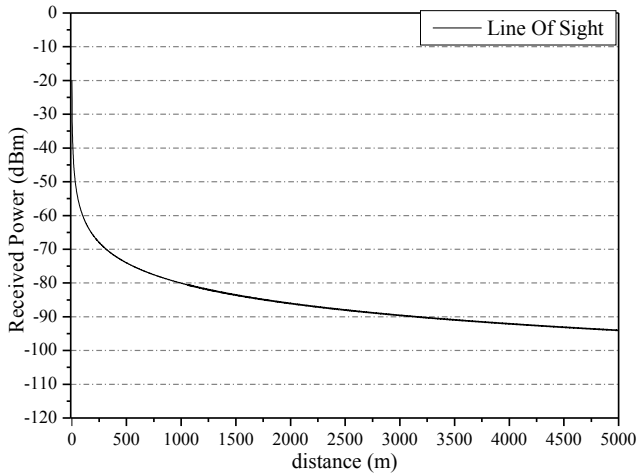


Figure 6: The total power of the LOS field vs. distance.

tennas), where the reflected fields for the two polarizations are correlated.

Due to the uncertainties introduced by foliage, the exact field cannot be evaluated deterministically. However, the magnitude of the received field can be modeled stochastically by the Rician probability density function (pdf):

$$f(x|\nu, \sigma) = \frac{x}{\sigma^2} e^{\left(\frac{-(x^2 + \nu^2)}{2\sigma^2}\right)} I_0\left(\frac{x\nu}{\sigma^2}\right), \quad (1)$$

where ν^2 is the power of the LOS path, $2\sigma^2$ is the average power of the other contributions x is the signal's amplitude and $I_0(z)$ is the modified Bessel function of the first kind and zero order. The cumulative distribution function (cdf), is given by:

$$F_x(x|\nu, \sigma) = 1 - Q_1\left(\frac{\nu}{\sigma}, \frac{x}{\sigma}\right), \quad (2)$$

where $Q_1(a, b)$ is the Marcum Q-function. Let γ denote the receiver's threshold. Then the probability of successful delivery of information from the transmitting antenna to the receiving antenna is:

$$P(X \geq \gamma) = 1 - F_x(\gamma|\nu, \sigma), \quad (3)$$

where $F_x(\gamma|\nu, \sigma)$ corresponds to the link-fail probability for the given receiver's threshold γ . Therefore, by defining ν and σ for each link, we can calculate the corresponding probability for successful communication. Equation (3) sizes the probability of successful communication among each pair of co-polarized antennas. As explained earlier, the corresponding probability for the other antenna-pair is expected to be independent and can be calculated similarly. The link from transmitter to receiver will fail if both orthogonally polarized links fail. Since the two pdfs are independent, the probability of failure of both links is simply given as the product of the probabilities of the two events. Let p_{ij}^+ denote the probability of failure of link between nodes i and j for the vertically polarized antennas and p_{ij}^* the corresponding probability for the horizontally polarized antennas. Then, the probability of failure of both antenna-pairs p_{ij}^f is:

$$p_{ij}^f = p_{ij}^+ p_{ij}^*, \quad (4)$$

and the two probabilities can be calculated by properly applying (2), as will be demonstrated in the following example.

2.1 Calculation of the link-fail probability

The power of the LOS field with respect to the transmit-receive distance is given in Figure 6. The transmitted power is set to the maximum EIRP, namely 20dBm and the gain of the receiving antenna is considered equal to 0dBi. As discussed earlier, the LOS power quantifies parameter ν^2 of the Rician pdf. Parameter $2\sigma^2$ is the average power of all scattered components; large σ indicates stronger scattered components. We define the k -factor [8] (k is the ratio between the power of the LOS component to the mean power of all scattered components expressed in dB); $k = 10 \log_{10}(\nu^2/2\sigma^2)$. Even though ν can be estimated for each link, assuming a given distance and receiving antenna gain, parameter k can only be set after extensive measurements in the actual network.

For example, assuming a distance of 4400m, a receiving antenna gain of 8dBi at the direction of the transmit antenna, then the expected received power of the LOS component will be -85dBm. Considering $k=3$ dB and the receiver's sensitivity equal to -90dBm, the probability of failure from the Rice distribution is 10.73%. Assuming the same conditions for the orthogonally polarized pair of antennas, the total link-fail probability, given by (4) is only 1.15%. Hence, an important performance gain is accomplished by the proposed polarization diversity scheme.

3. INFORMATION FLOW

Finally, we implement 120° sector antennas, so that each node can communicate with several other nodes (instead of a single P2P link), in order to increase the possible paths for information-flow. The exact direction of each antenna-pair, installed on each node is shown in Figure 1. All antennas are installed so that the 3dB horizontal beamwidth of the antennas illuminates the possible nodes of the network that satisfy the necessary LOS conditions. Therefore a maximum of 6dBs are lost from the dynamic range of each transmit-receive pair (assuming that a pair communicates at the margins of the 3dB beamwidth of the antenna pattern). To evaluate the performance enhancement from this strategy, all possible paths linking each node with the backbone network (either of nodes b_1, b_2, b_3 in Figure 1) are calculated. Such an example is illustrated in Figure 7, where all possible paths from node n_1 to the backbone network are shown.

The entire process for the calculation of the outage probability, i.e., the probability that its transmitted information (e.g. sensor's signal) never reached the backbone network, of node n_1 is demonstrated in a step-by-step process. After creating the original tree diagram connecting n_1 to the backbone (step 1 in Figure 7), we start simplifying the diagram from right to left (from the backbone towards the node). Initially at step 2, we calculate the link-fail probability from node n_4 towards the backbone. Since we have two branches in parallel, namely n_4b_3 and n_4b_2 , the fail probability from n_4 to the backbone demands that both links fail; therefore, it equals the product of the two probabilities (independent variables): $p_{n_4b}^f = p_{n_4b_3}^f p_{n_4b_2}^f$. The initial two branches from n_4 are substituted in step 2 by a single branch with the calculated link-fail probability. In the next step

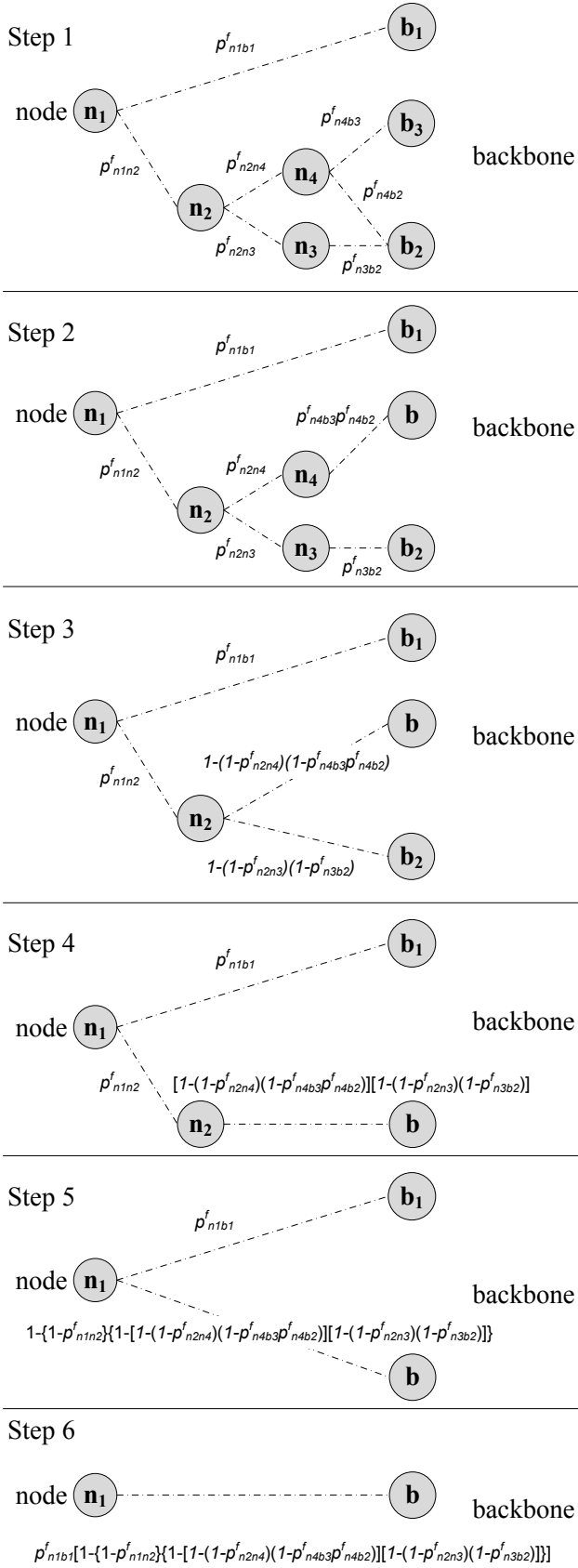


Figure 7: Logical diagram of the information flow from node n_1 towards the backbone network.

(Step 3), we continue the simplification, with the branches $n_2 n_4, n_4 b$ connected in series. Since they are connected in series, information from node n_2 reaches the backbone only if both links are successful. The probability that both links are successful is denoted by the "s" superscript and is given by $p_{n_2 b}^s = p_{n_2 n_4}^s p_{n_4 b}^s = (1 - p_{n_2 n_4}^f)(1 - p_{n_4 b}^f)$, where $p_{n_4 b}^f$ was calculated earlier. The corresponding fail probability for the two serially connected branches is simply $p_{n_2 b}^f = 1 - p_{n_2 b}^s$. A similar process is demonstrated in "Step 3" of Figure 1 for the other two serially connected branches from n_2 , namely $n_2 n_3$ and $n_3 b_2$. We continue the same process until we reach node n_1 . The outage probability $P_{n_1}^f$ of node n_1 , assuming a maximum number of three (3) hops, is given by:

$$P_{n_1}^f = p_{n_1 b_1}^f \left[1 - p_{n_1 n_2}^s [1 - (1 - p_{n_2 n_3}^s p_{n_3 b_2}^s) \times [1 - p_{n_2 n_4}^s (1 - p_{n_4 b_2}^f p_{n_4 b_3}^f)]] \right]. \quad (5)$$

In order to calculate the achieved improvement for each node, we must calculate separately the link-fail probabilities of all involved P2P links. Such procedure is summarized in Fig. 7. The expected LOS reception power level sizes in Fig. 7. The expected LOS reception power level sizes in a Rician distribution with $k=3$ dB and receiver's sensitivity equal to -90 dBm. By substituting in (5) all probabilities of the links, considering their distances, the antenna radiation patterns and a maximum EIRP of 20 dBm, the outage probability of node n_1 is reduced to only $1.43 \times 10^{-5}\%$ from 10.73% , which is the corresponding failure-probability considering a single P2P link from n_1 to b_1 without diversity.

3.1 Power consumption of the network

As discussed earlier, the network is designed so that redundant routing paths are available for the information flow. Due to the large distances separating all nodes, transmission power is always set to its maximum, that is 20 dBm EIRP. Therefore, from a power consumption perspective the path with the fewest hops is selected first for transmitting the sensor's data. Therefore, in the analyzed example of node n_1 , sensor data is initially transmitted through link $n_1 b_1$. If that link fails, all alternative paths have the same number of hops (3). The one with the smallest failure-probability is selected next ($n_1 n_2 n_4 b_3$) and so on.

4. CONCLUSION

Overall, this work put forward intelligent methods, to ensure information-flow of a wireless long-distance water-management network against fading effects. We proposed the implementation of orthogonally polarized sector antennas, greatly improving the probability of successful reception among any two nodes of the network, while also increasing the number of routing paths. Therefore, overall reliability performance is improved.

5. ACKNOWLEDGMENTS

This work was supported by the SYN11-6-925 AquaNet project, which is executed within the framework of the "Cooperation 2011" program of the Greek General Secretariat for Research & Technology (GSRT), funded through European Union and national funds. The authors thank the

Table 1: Calculation of link-probabilities for the evaluation of the outage probability of node n_1

link	distance (km)	LOS-Rx (dBm)	p_{Rice}^f	Diversity p^f
$n_1 - b_1$	4.41	-85	0.107	0.012
$n_1 - n_2$	0.69	-73	0.006	3×10^{-5}
$n_2 - n_3$	1.7	-84	0.082	0.007
$n_3 - b_2$	4.95	-86	0.14	0.02
$n_2 - n_4$	1.98	-81	0.04	0.001
$n_4 - b_2$	4.75	-86	0.14	0.02
$n_4 - b_3$	1.72	-83	0.06	0.004

research personnel of the Telecommunication Systems Research Institute (Technical University of Crete, Greece) for their assistance in conducting this research.

6. REFERENCES

- [1] T. Tamir. On radio-wave propagation in forest environments. *IEEE Transactions Antennas & Propagation*, 15(6):806–817, November 1967.
- [2] S. Swarup, R. Tewari Depolarization of radio waves in jungle environment. *IEEE Transactions Antennas & Propagation*, 27(1):113–116, January 1979.
- [3] Il-Suek Koh, K. Sarabandi. Polarimetric channel characterization of foliage for performance assessment of GPS receivers under tree canopies. *IEEE Transactions Antennas & Propagation*, 50(5):713–726, August 2002.
- [4] Recommendation ITU-R P.833-5. *Attenuation in vegetation*. Tech. Rep. P.833-2, ITU, Geneva, Switzerland, 2005.
- [5] S. A. Torrico, H. L. Bertoni, R. H. Lang. Modeling tree effects on path loss in a residential environment. *IEEE Transactions Antennas & Propagation*, 46(6):872–880, June 1998.
- [6] T. S. Rappaport. *Wireless Communications: Principles and Practice*. Prentice Hall, 2nd Ed., 2002.
- [7] S. O. Rice. Mathematical analysis of random noise. *Bell System Technical Journal*, 24:46–156, 1945.
- [8] L. J. Greenstein, S. S. Ghassemzadeh, V. Erceg, and D. G. Michelson. Ricean K-factors in narrow-band fixed wireless channels: theory, experiments, and statistical models. *IEEE Transactions Vehicular Technology*, 58(8):4000–4012, October 2009.